

7

## 3 Physically based evaluation of climate models 4 over the Iberian Peninsula

5 Ma. del Carmen Sánchez de Cos Escuín ·  
6 Jose Ma. Sánchez-Laulhé · Carlos Jiménez Alonso ·  
7 Juan Manuel Sancho Ávila · Ernesto Rodríguez-Camino

8 Received: 8 February 2012 / Accepted: 29 November 2012  
9 © Springer-Verlag Berlin Heidelberg 2012

10 **Abstract** A novel approach is proposed for evaluating  
11 regional climate models based on the comparison of  
12 empirical relationships among model outcome variables.  
13 The approach is actually a quantitative adaptation of the  
14 method for evaluating global climate models proposed by  
15 Betts (Bull Am Meteorol Soc 85:1673–1688, 2004). Three  
16 selected relationships among different magnitudes involved  
17 in water and energy land surface budgets are firstly  
18 established using daily re-analysis data. The selected  
19 relationships are obtained for an area encompassing two  
20 river basins in the southern Iberian Peninsula correspond-  
21 ing to 2 months, representative of dry and wet seasons. The  
22 same corresponding relations are also computed for each of  
23 the thirteen regional simulations of the ENSEMBLES  
24 project over the same area. The usage of a metric based on  
25 the Hellinger coefficient allows a quantitative estimation of  
26 how well models are performing in simulating the relations  
27 among surface magnitudes. Finally, a series of six rankings  
28 of the thirteen regional climate models participating in the  
29 ENSEMBLES project is obtained based on their ability to  
30 simulate such surface processes.

31  
32 **Keywords** Climate models · Evaluation

A1 Ma. del Carmen Sánchez de Cos Escuín ·  
A2 J. Ma. Sánchez-Laulhé · C. J. Alonso · J. M. S. Ávila  
A3 AEMET, Centro Meteorológico de Málaga, Demóstenes 4,  
A4 29010 Málaga, Spain

A5 E. Rodríguez-Camino (✉)  
A6 AEMET, Servicios Centrales, Leonardo Prieto Castro 8,  
A7 28040 Madrid, Spain  
A8 e-mail: erodriguezc@aemet.es

### 1 Introduction

Climate models are numerical representations of the cli- 34  
mate system based on the physical, chemical, and biolog- 35  
ical properties of its components, their interactions and 36  
feedback processes. Different climate models constitute 37  
multiple realizations of the climate system based on com- 38  
puter programs. Climate models differentiate among them 39  
by the approximations and discretizations used to solve the 40  
mathematical equations representing its physics, chemistry 41  
and biology. Although climate models continue to have 42  
significant limitations which lead to uncertainties in the 43  
magnitude and timing, as well as regional details, they have 44  
consistently provided a robust and unambiguous picture of 45  
the climate system. There is currently a considerable con- 46  
fidence in the simulations provided by climate models due 47  
to the fact that model principles are based on well estab- 48  
lished physical laws, such as conservation of mass, energy 49  
and momentum. An additional source of confidence is their 50  
ability to simulate important aspects of the current and past 51  
climates, as well as their changes (Randall et al. 2007). 52

The climate system includes a variety of physical pro- 53  
cesses, such as cloud processes, radiative processes and 54  
boundary-layer processes, which interact with each other 55  
on many temporal and spatial scales. Due to the limited 56  
resolutions of the models, many of these processes are not 57  
resolved adequately by the model grid and must therefore 58  
be parameterized. As confidence in global models decrea- 59  
ses at smaller scales, higher resolution regional climate 60  
models (RCMs) provide quantitative value to climate 61  
simulations. With finer resolution, mesoscale phenomena, 62  
contributing e.g. to intense precipitation, and coupling 63  
between regional circulations and convection can be 64  
resolved. Higher resolution RCMs also include other types 65  
of scale-dependent variability such as extreme winds and 66

67 locally extreme temperature that coarse-resolution global  
68 models will smooth. Regional-scale simulations also have  
69 phenomenological value, being able to represent processes  
70 that global models either cannot resolve or can resolve only  
71 poorly (CCSP 2008).

72 As climate models are very complex systems, they have  
73 different capabilities and limitations which can be evalu-  
74 ated using a variety of methods and approaches. Models  
75 can be tested either globally at the system-level or at  
76 component-level. Whereas system-level evaluation is  
77 focused on the outputs of the full model, component-level  
78 evaluation isolates particular components of the model  
79 (e.g. atmosphere, ocean, land surface, etc.) or even sub-  
80 components (e.g., numerical methods, parameterizations of  
81 different physical processes, etc.) to test them independ-  
82 ently of the complete model. A hybrid approach consists  
83 of evaluating the whole system but putting the focus on  
84 some specific process or component. For example, we may  
85 be interested in exploring how well climate models are able  
86 to simulate surface processes or interaction between land  
87 and atmosphere (Randall et al. 2007).

88 A number of metrics have been designed to compare  
89 quantitatively climate model simulations against past or  
90 current observed climates. Although many different met-  
91 rics of model reliability have been proposed (see, e.g.,  
92 Gleckler et al. 2008) there is at present little consensus on a  
93 particular metric to discriminate “good” and “bad”  
94 models. In fact, the main issue is the virtually infinite  
95 number of metrics that can be defined, being each of them  
96 appropriate for different purposes (Knutti et al. 2010).  
97 Land-surface processes and interaction between land-sur-  
98 face and atmosphere are especially relevant for the evalu-  
99 ation of climate models simulations as they are very much  
100 responsible for precipitation and surface temperature,  
101 which traditionally have been used to define local climate.  
102 The performance of a climate model when simulating the  
103 interaction between land-surface and atmosphere depends  
104 critically on the correct coupling between land-surface  
105 fluxes and state variables (e.g., evapotranspiration, sensible  
106 heat flux, radiative fluxes, soil moisture, etc.). Some  
107 researchers (e.g., Betts 2004, 2007; Betts et al. 2006; Jaeger  
108 et al. 2009; Santanello et al. 2009; Seneviratne et al. 2010)  
109 have pointed out that an alternative way to identify cou-  
110 pling between related variables is to derive empirical  
111 relationships by displaying the investigated variables as a  
112 function of one another. These relationships can only be  
113 suggestive of coupling mechanisms at the land–atmosphere  
114 interface without pointing to any direction of causality. As  
115 these relationships can be derived for both observations  
116 and model data, they are also of strong relevance for model  
117 evaluation. We extend in this paper the method for eval-  
118 uating global climate models proposed by Betts (2004) to  
119 RCMs including as main novelties, first, the quantification—

by introducing the Hellinger distance—of how well dif- 120  
ferent pairs of empirical relationships are represented by 121  
models and, second, the usage of such metric to evaluate 122  
and rank models according to accuracy of their simulation 123  
of atmosphere/land surface coupling. 124

125 In recent years a large number of RCM simulations have  
126 been produced for simulating the future European climate  
127 (e.g. Christensen and Christensen 2007; Déqué et al. 2005,  
128 2007; van der Linden and Mitchell 2009). As indicated by  
129 Kjellström and Giorgi (2010), a relevant finding in these  
130 multi-model experiments is that climate change scenarios  
131 with different RCMs can differ significantly, even if the  
132 lateral boundary conditions are taken from the same global  
133 climate model. Therefore, an additional level of uncertainty  
134 to the total uncertainty is added by the downscaling process  
135 associated to regional climate change simulations. In order  
136 to explore such uncertainties, it is reasonable to make use  
137 of multi-model ensembles of RCMs for deriving detailed  
138 climate change information at the regional scale. It can  
139 even be envisaged the application of some kind of per-  
140 formance-based weighting schemes in the process of  
141 combining multi-model results, to increase the reliability of  
142 the projections (Giorgi and Mearns 2002). In the European  
143 project ENSEMBLES (van der Linden and Mitchell 2009),  
144 a work package was devoted to designing and testing a  
145 weighting system for a multi-model ensemble of RCMs.  
146 Kjellström and Giorgi (2010) have described the set of  
147 metrics derived in the framework of the ENSEMBLES  
148 project to combine RCMs simulations based on their per-  
149 formance and aiming at the production of probabilistic  
150 climate change projections (see also Climate Research,  
151 Special Issue No 23 2010 on ‘Regional Climate Model  
152 evaluation and weighting’). Christensen et al. (2010) have  
153 explored six metrics designed to capture different aspects  
154 of RCM performance in reproducing large-scale circulation  
155 patterns, meso-scale signals, daily temperature and pre-  
156 cipitation distributions and extremes, trends and the annual  
157 cycle. Most of their explored metrics were based on the  
158 performance of different aspects of temperature and pre-  
159 cipitation fields but none of them relied on the correctness  
160 of physical processes simulations.

161 Within this frame our method proposes an evaluation of  
162 the interaction between land and atmosphere simulated by  
163 regional climate models as a complement to the above  
164 described methods to measure the performance of RCMs.  
165 The method here described characterizes the differences or  
166 distances of two 2D-scattered plots describing the empiri-  
167 cal relationship linking pairs of land surface variables by  
168 making use of the Hellinger coefficient (Cramer 1946). The  
169 Hellinger coefficient—initially introduced in probability  
170 and statistics theories to measure the closeness of two  
171 probability distribution functions—will therefore allow us  
172 to quantify how close the same empirical relation obtained

173 from a climate model simulation and from observation are.  
174 In order to compare the here proposed method of evaluation  
175 based on the interaction between land and atmosphere  
176 with the six metrics proposed by Christensen et al. (2010),  
177 we have computed the Hellinger coefficient for the pair  
178 temperature and precipitation (T2m–PP) and also standard  
179 scores for temperature and precipitation.

180 ERA-Interim re-analysis (Dee et al. 2011) has been used  
181 as a proxy of actual observations for the selected surface  
182 magnitudes due to the lack of spatial coverage of obser-  
183 vations for most of the fluxes and surface variables con-  
184 sidered here. Direct measures of fluxes and surface/soil  
185 variables are frequently restricted to a few reference  
186 observatories or recent satellite measurements. Data  
187 assimilation algorithms provide a full and consistent 3D  
188 representation of the atmosphere constrained by the avail-  
189 able observations and physical relationships among vari-  
190 ables describing the state of the atmosphere. The  
191 four-dimensional variational data assimilation used in  
192 ERA-Interim includes, apart of the relationships of the  
193 forecast model, those of the complex statistical balance  
194 between the first guess error variables. We are fully aware  
195 that fluxes—and certain variables not directly observed—  
196 provided by a re-analysis are very much dependent on the  
197 constraints imposed by the data assimilation algorithm and  
198 the underlying model. Variables not directly observed are  
199 mainly produced by the underlying forecasting model. In  
200 fact, it may happen that fluxes and non-analysed soil/sur-  
201 face variables show bias attributable to the inaccuracies of  
202 the assimilation procedure. Therefore, before using re-  
203 analysis data as reference or ground-truth some efforts  
204 must be devoted to verify this assumption for the variables,  
205 region and seasons selected. Nevertheless, it should be  
206 stressed that this paper focuses on the proposed method to  
207 evaluate model outputs based on empirical relationship  
208 linking pairs of surface relevant magnitudes and not on a  
209 comprehensive validation of the reference.

210 Once the selected relationships have been determined  
211 for the ERA-Interim re-analysis data, the corresponding  
212 relationships are also determined for each of the thirteen  
213 regional simulations of the ENSEMBLES project (van der  
214 Linden and Mitchell 2009) using daily data over the same  
215 area. Finally, a measure of the closeness based on the  
216 Hellinger coefficient is applied to produce a ranking of  
217 the thirteen regional climate models participating in the  
218 ENSEMBLES project focused mainly on their ability to  
219 simulate surface processes.

220 The paper is organized as follows. Section 2 describes  
221 the data sets used in this study. The ground truth from  
222 ERA-Interim re-analysis is evaluated in Sect. 3. The prin-  
223 ciples, advantages and limitations of the method are  
224 described in Sect. 4. Main results are presented in Sect. 5.  
225 Finally, conclusions are summarized in Sect. 6.

## 2 Data

226  
227 The ERA-Interim re-analysis data (Dee et al. 2011) has  
228 been used through the whole study as a reference to  
229 compare with RCMs outputs. Although it can be argued  
230 that some soil/surface variables and surface fluxes provided  
231 by a re-analysis are not the ideal reference to be used as an  
232 accurate representation of the observed atmosphere and/or  
233 land surface, it is however a practical approach which  
234 circumvents the problem of the insufficient spatial cover-  
235 age of in situ data and of the inaccuracy of satellite data for  
236 certain surface variables. It must be always kept in mind  
237 that fluxes values correspond to 12 h forecasting and  
238 therefore they are very much dependent on the underlying  
239 model.

The following data have been used for this study: 240

- (a) Daily analysis (0000, 0600, 1200, 1800 UTC) from 241  
1989 to 2008 of Skin Temperature (SKT) and 2-meter 242  
Temperature (T2m) and daily averaged 12 h forecasts 243  
(0000, 1200 UTC) of Surface Net Thermal Radiation 244  
( $LW_{net}$ ), Surface Net Solar Radiation ( $SW_{net}$ ), Surface 245  
Sensible Heat Flux (SSHF) and Total Precipitation 246  
(PP) from the European Centre for Medium-Range 247  
Weather Forecast (ECMWF) ERA-Interim reanalysis 248  
(Dee et al. 2011). The ERA-Interim atmospheric 249  
model is configured with 60 levels in the vertical; a 250  
T255 spherical-harmonic representation for the basic 251  
dynamical fields and a reduced Gaussian grid with 252  
approximately uniform 79 km spacing for surface and 253  
other grid-point fields. 254
- (b) Daily fields from 1991 to 2000 of Maximum Soil 255  
Temperature ( $T_{smx}$ ), Minimum Soil Temperature 256  
( $T_{smn}$ ) and 2-m Temperature (T2m), and daily 257  
averaged fields of Surface Net Thermal Radiation 258  
( $LW_{net}$ ), Surface Net Solar Radiation ( $SW_{net}$ ), Sur- 259  
face Sensible Heat Flux (SSHF) and Precipitation 260  
(PP) from the thirteen RCMs participating in the 261  
Research Theme 3 (RT3) of the ENSEMBLES 262  
project (van der Linden and Mitchell 2009). All 263  
regional simulations for the period 1991–2000 were 264  
driven by ERA-40 reanalysis (Uppala et al. 2005). 265  
Table 1 provides information of the 13 models 266  
considered in this study: institution, model, number 267  
of vertical levels and key references. The fields were 268  
obtained from the ENSEMBLES RT3/RT2B data 269  
archive (<http://ensemblesrt3.dmi.dk>). 270

271 Only the months of July and November corresponding  
272 to ERA-Interim and RT3-ENSEMBLES data have been  
273 used. The election is justified by the fact that July is rep-  
274 resentative of the dry season, whereas November is  
275 representative of the wet season over Southern Spain.  
276 ERA-Interim and all 13 RT3-ENSEMBLES regional

**Table 1** List of regional climate models participating in the EU-FP6 ENSEMBLES project

Institution	RCM	Vertical levels	Reference
CHMI	ALADIN	31	N/A
C4I	RCA3	31	Kjellström et al. (2005)
DMI	HIRHAM	31	Christensen et al. (2007)
ETHZ	CLM	32	Böhm et al. (2006)
HC	HadRM3Q0	19	Collins et al. (2006)
HC	HadRM3Q3	19	Collins et al. (2006)
HC	HadRM3Q16	19	Collins et al. (2006)
KNMI	RACMO	40	Van Meijgaard et al. (2008)
METNO	HIRHAM	31	Haugen and Haakensatd (2006)
MPI	REMO	27	Jacob (2001)
SHMI	RCA	24	Kjellström et al. (2005)
UCLM	PROMES	28	Sánchez et al. (2004)
OURANOS	CRCM	29	Plummer et al. (2006)

**Fig. 1** Selected area for the study of ERA-Interim re-analysis and ENSEMBLES datasets

277 models datasets have been interpolated to a common grid  
 278 (0.25° latitude × 0.25° longitude) defined by a rectangular  
 279 area (from 40.5°N to 37.5°N, and from 7.0°W to 2.0°W)  
 280 covering part of Tagus and Guadiana river basins in  
 281 southern Iberian Peninsula (see Fig. 1).

### 282 3 Evaluation of ground-truth ERA-Interim data

283 Although the quality of ERA-Interim is not the subject of  
 284 this paper, its selection as ground-truth requires of previous  
 285 discussion and some validation against in situ and satellite  
 286 observations. In particular, the quality of the ERA-Interim  
 287 selected fluxes ( $LW_{net}$ ,  $SW_{net}$  and  $SSHf$ ) must be carefully  
 288 validated—as these quantities are not analyzed—before  
 289 accepting them as ground-truth reference to compare  
 290 against the corresponding quantities from regional climate  
 291 models. The validation of ERA-Interim fluxes implies a  
 292 certain degree of difficulty as the corresponding observa-  
 293 tional satellite data, mainly from EUMETSAT Satellite  
 294 Application Facility on Climate Monitoring (CM SAF)  
 295 products (see <http://www.cmsaf.eu>) are available only for  
 296 recent years and these last data do not overlap in time with  
 297 RT3-ENSEMBLES regional models simulations.

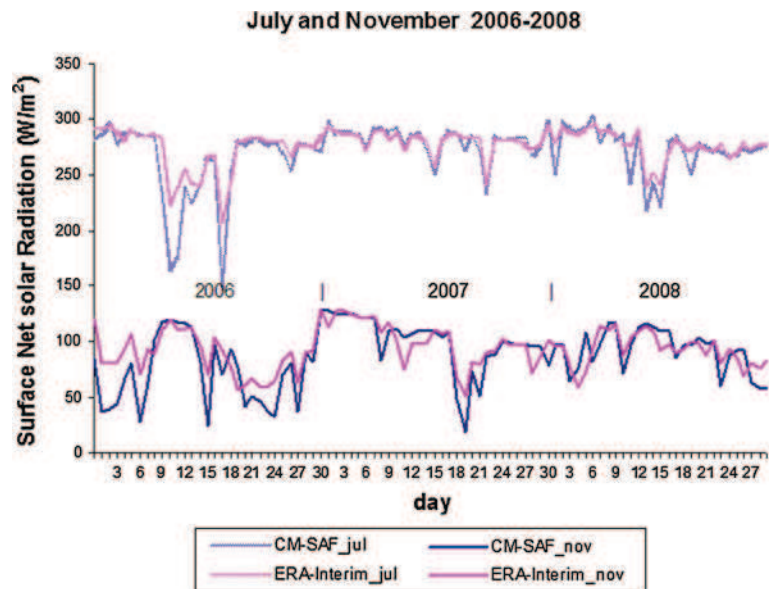
298 For the evaluation of  $LW_{net}$  and  $SW_{net}$ , we have made  
 299 use of CM SAF products. The CM SAF data products are  
 300 categorized in monitoring data sets obtained in near real  
 301 time and data sets based on carefully inter-sensor calibrated  
 302 radiances. The homogenous sets of high-quality data are  
 303 derived from several instruments on-board meteorological  
 304 operational satellites in geostationary and polar orbit as the

Meteosat and EUMETSAT Polar System satellites, 305  
 respectively. Surface radiation products are retrieved from 306  
 SEVIRI/GERB instruments on MSG satellite and AVHRR 307  
 instruments on METOP and NOAA satellites. They are 308  
 available as gridded monthly and daily means data at 309  
 15 × 15 km resolution. 310

Figure 2 shows the comparison of daily  $SW_{net}$  obtained 311  
 from ERA-Interim and from CM SAF averaged for the 312  
 same area and for the months of July and November cor- 313  
 responding to years 2006, 2007 and 2008. The figure shows 314  
 a remarkable coincidence between ERA-Interim and CM 315  
 SAF values for clear sky days. Cloudy days show a ten- 316  
 dency of ERA-Interim  $SW_{net}$  to have higher values than the 317  
 corresponding CM SAF ones. The mean absolute differ- 318  
 ence (MAD) between both curves is 7.52 and 13.52  $Wm^{-2}$  319  
 for July and November, respectively (see red lines in 320  
 Fig. 4). The lower value for July is mainly due to the 321  
 predominance of clear sky conditions. Computation of 322  
 MAD between the ENSEMBLES regional models and 323  
 ERA-Interim show clearly larger values (see box plots in 324  
 Fig. 4) and therefore it can be reasonably assumed that 325  
 ERA-Interim  $SW_{net}$  is a good approximation for the 326  
 observed reference. As data available from ENSEMBLES 327  
 RCMs do not cover the period 2006–2008, we have instead 328  
 compared ERA-Interim against each of the ENSEMBLES 329  
 regional models for the months of July and November of 330  
 years 1998, 1999 and 2000 (see Fig. 4). 331

Unfortunately, there is no daily data available from CM 332  
 SAF for  $LW_{net}$ . Therefore, the evaluation of ERA-Interim 333  
 $LW_{net}$  will be based on monthly averages. Figure 3 depicts 334  
 monthly mean  $LW_{net}$  obtained from ERA-Interim and from 335  
 CM SAF averaged for the same area and for years 336  
 2006–2010. The mean absolute difference between both 337

**Fig. 2** Daily 12 h mean Surface Net Solar Radiation ( $SW_{net}$ ) averaged over the selected area (see Fig. 1) from ERA-Interim and CM-SAF data for 3 months of July and November corresponding to years 2006–2008



338 curves is  $4.67 \text{ Wm}^{-2}$  for the whole period. Again, the  
 339 corresponding computation of MAD between each of the  
 340 13 RT3-ENSEMBLES regional models and ERA-Interim  
 341 show clearly larger values (see box plots in Fig. 4), but for  
 342 the period 1996–2000, and therefore it can be reasonably  
 343 assumed than ERA-Interim  $LW_{net}$  is a good approximation  
 344 for the observed reference.

345 For the evaluation of SSHF we have to rely on in situ  
 346 observations from a number of flux tower networks (Kráľ  
 347 2011). This evaluation made use of the 2006 data from the  
 348 FLUXNET LaThuile Synthesis dataset which compiles  
 349 flux tower eddy-covariance measurements from a number  
 350 of regional flux tower networks across the globe (Baldocchi  
 351 et al. 2001). Root mean square error of ERA-Interim SSHF  
 352 compared against FLUXNET daily data for the whole 2006  
 353 show values ranging from 20 to  $40 \text{ Wm}^{-2}$  for most West-  
 354 ern European towers, values are generally lower than the  
 355 corresponding rmse of regional models computed with  
 356 respect to ERA-Interim SSHF. This is an expected result,  
 357 consequence of the land surface analysis combining syn-  
 358 optic observations over land with background estimates  
 359 based on 6-hourly estimates of screen-level temperature  
 360 and dew point from the latest atmospheric analysis (Dou-  
 361 ville et al. 1998). The analysis increments for screen-level  
 362 temperature and humidity are subsequently used to update  
 363 soil moisture and soil temperature estimates for each of the  
 364 four layers of the land-surface model, by a simple empir-  
 365 ical approach (Douville et al. 2000; Mahfouf et al. 2000).  
 366 Therefore, surface sensible and latent fluxes are con-  
 367 strained in ERA-Interim by soil moisture and soil tem-  
 368 perature which in turn are corrected by screen-level  
 369 temperature and humidity observations.

#### 4 Methodology

371 Atmosphere and land surface are strongly coupled sub-  
 372 systems of the climate system. Surface fluxes (of energy,  
 373 water, momentum, carbon, etc.) enable the coupling of  
 374 both sub-systems. In fact, climate variables, as e.g. surface  
 375 equilibrium temperature, diurnal temperature range, near  
 376 surface air temperature and humidity, are very dependent  
 377 on surface fluxes. Moreover, the entire structure and fea-  
 378 tures of the atmospheric boundary layer are in turn very  
 379 influenced by land-surface and atmosphere coupling  
 380 expressed in the form of surface fluxes (see, e.g., Stensrud  
 381 2007). Whenever we refer in this paper to coupling  
 382 between two variables, we mean that one variable controls  
 383 each other (following Seneviratne et al. (2010)) or even  
 384 better that both are forced to change together in a way  
 385 prescribed by the underlying processes. For example, for  
 386 the particular case of the pair of variables  $SW_{net} - LW_{net}$ ,  
 387 Figure 6 shows that  $SW_{net}$  increases whenever  $LW_{net}$   
 388 increases (and vice versa) for November days, whereas this  
 389 is only true when  $SW_{net}$  does not reach the maximum value  
 390 (generally reduced by clouds) for July days. This coupling  
 391 does not necessarily mean that the relationship between  
 392 both variables is linear. In fact, in most of the cases, the  
 393 relationship is linear only as a first approximation. The  
 394 level of dispersion shown by 2D-scattered plots indicates—  
 395 without any expression of causality—how tight the rela-  
 396 tionship between pairs of variables is.

397 Surface fluxes involved in the surface energy budget are  
 398 especially relevant for land-surface and atmosphere cou-  
 399 pling. The surface energy budget equation can be expressed  
 400 in a simplified form as:

**Fig. 3** Monthly mean Surface Net Thermal Radiation ( $LW_{net}$ ) averaged over the selected area (see Fig. 1) from ERA-Interim and CM-SAF data for years 2006–2010. Months of July and November are additionally marked by symbols

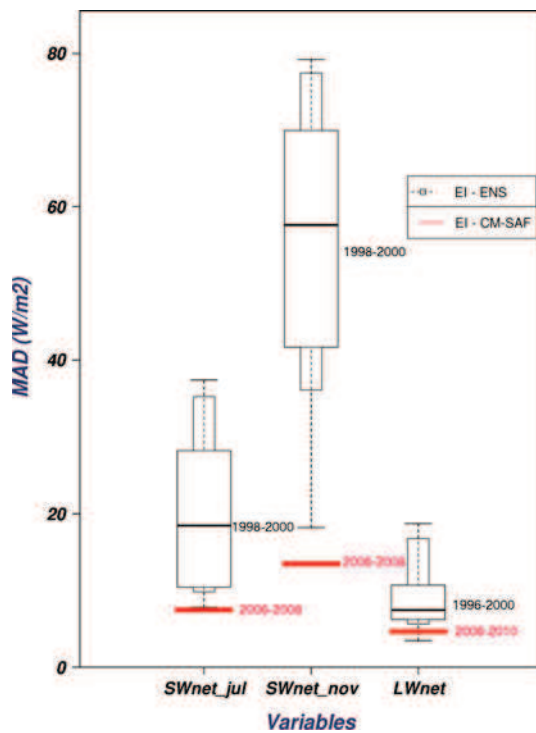
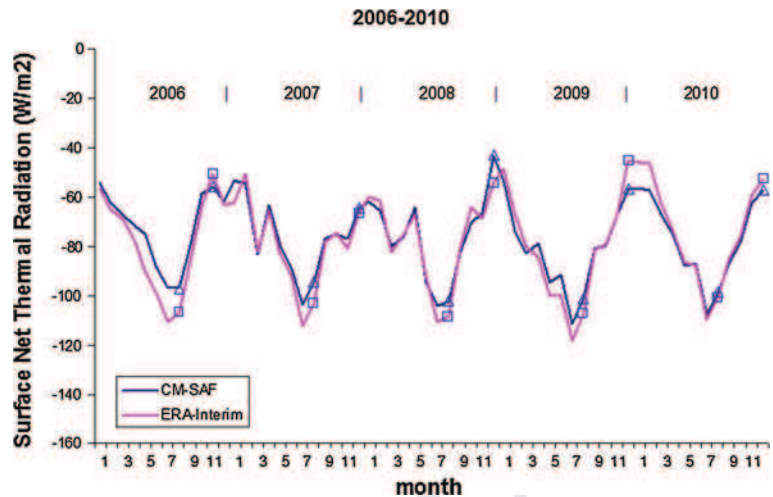


**Fig. 4** Mean absolute difference of Net Solar Radiation fluxes averaged over the selected area from CM-SAF data (red) and thirteen ENSEMBLES RCMs (box plot) with respect to ERA-Interim. Daily Surface Net Solar Radiation ( $SW_{net}$ ) for the months of July (left) and November (centre) and monthly Surface Net Thermal Radiation ( $LW_{net}$ ) (right) are represented for the periods shown. Box plots represent the minimum, maximum, median and 10th, 25th, 75th and 90th percentiles

$$R_{net} = SW_{net} + LW_{net} = SSHF + SLHF + G \quad (1)$$

402 The net surface radiation,  $R_{net}$ , is the sum of net shortwave  
 403 ( $SW_{net}$ ) and longwave ( $LW_{net}$ ) fluxes;  $R_{net}$  is balanced by  
 404 the upward sensible heat flux (SSHF) the upward latent

heat flux (SLHF) and the storage (G) (neglected on daily 405  
 scales). Both heat fluxes are the important mechanisms to 406  
 turn energy back into the atmosphere from land surface. 407  
 Accuracy and minimal drift in the land-surface climate and 408  
 the surface fluxes impact forecast skill on all timescales 409  
 (Betts 2009; Stensrud 2007). 410

The surface  $LW_{net}$  plays a fundamental role in land- 411  
 atmosphere coupling. Although upward and downward  $LW$  412  
 fluxes are strongly dependent functions of temperature, 413  
 however,  $LW_{net}$  is largely determined by humidity and 414  
 cloud cover on daily-mean timescales, due to the strong 415  
 vertical coupling of the atmospheric temperature and 416  
 moisture structure. For example, the depth of the daytime 417  
 adiabatic mixed layer (ML) is a function of relative 418  
 humidity (RH). Outgoing  $LW_{net}$  decreases as near-surface 419  
 RH rises (and mean cloud-base falls), and decreases as 420  
 cloud cover increases.  $LW_{net}$  plays in turn a fundamental 421  
 role in the diurnal cycle over land. For example, a clear dry 422  
 atmosphere gives place to an increased outgoing  $LW_{net}$  423  
 associated with surface cooling, lower minimum surface 424  
 temperature at night and very stable nocturnal boundary 425  
 layer, NBL. In terms of the daily climate, the strength of 426  
 the NBL is closely related to the diurnal temperature range, 427  
 DTR (defined as  $DTR = T_{max} - T_{min}$ , where  $T_{max}$ ,  $T_{min}$  428  
 are the maximum and minimum values of 2-m Tempera- 429  
 ture). In the dry season, both atmospheric water vapour and 430  
 cloud cover reach relatively low values and therefore the 431  
 lifting condensation level (LCL) tends to reach relatively 432  
 higher values, contributing all these factors to an increased 433  
 outgoing  $LW_{net}$  (Betts 2009). 434

Surface water budget is also associated to energy bud- 435  
 get, as latent heat flux, caused by evapotranspiration, plays 436  
 an important role in both water and energy budgets. The 437  
 surface water budget can be expressed as: 438

$$\delta S / \delta t = P - E - R \quad (2)$$

440 where  $S$  stand for terrestrial water storage,  $P$  for total  
441 amount of precipitation,  $E$  for evapotranspiration and  $R$  for  
442 total runoff.

443 The relative importance of latent and sensible heat  
444 fluxes depends strongly on surface features. In bare, dry  
445 soils, the absorbed radiative energy is mostly used to heat  
446 the surface, turning back energy to the atmosphere usually  
447 as a vigorous, turbulent sensible flux. On the other hand,  
448 densely vegetated surfaces with enough water available for  
449 evapotranspiration invest most of the radiative energy in  
450 extracting subsurface water through the root system. This  
451 process of transpiration is mainly controlled by leaves,  
452 opening and closing their stomata according to the envi-  
453 ronmental conditions and to the available soil wetness.  
454 Transpiration turns energy back to the atmosphere in form  
455 of latent heat flux. Over land the availability of water  
456 essentially determines evaporative fraction,  $EF$ , (being  
457 defined as  $SLHF/(SLHF + SSHF)$ ). Soil water has a pri-  
458 mary role in the surface energy partition between latent and  
459 sensible heat fluxes, and in turn in the diurnal cycle of 2-m  
460 Temperature and humidity. The latent and sensible heat  
461 fluxes play a different role for the atmosphere. Sensible  
462 heat at the bottom means energy immediately available to  
463 the atmosphere, and contributes to the heating and/or  
464 deepening of the planetary boundary layer. For an entire  
465 atmospheric column, the net radiative cooling is balanced  
466 by energy involved in phase changes inside the column  
467 (condensation of water vapour and evaporation of rain) and  
468 sensible heat flux at the surface (see, e.g., Garratt 1992;  
469 Stensrud 2007).

470 The three following relationships involving surface  
471 fluxes and temperatures were selected in order to evaluate  
472 the performance of the RT3-ENSEMBLE regional models  
473 when simulating atmosphere land-surface coupling:

- 474 •  $SW_{net} - LW_{net}$ ,
- 475 •  $SW_{net} - SSHF$ ,
- 476 •  $LW_{net} - (T_{smx} - T_{smn})$ .

477 The variables selected are readily available both from  
478 ERA-Interim and RT3-ENSEMBLE datasets and, as dis-  
479 cussed above, are responsible and descriptive of different  
480 aspects related with energy and water budgets and with  
481 features of the atmospheric boundary layer.

482 The study area was selected inland of the Iberian Pen-  
483 insula to avoid potential influences of the coast. The area  
484 encompassing two river basins—Tagus and Guadiana—  
485 also shows approximate homogeneity with respect to soil,  
486 vegetation and climate being predominantly flat. The  
487 selected area belongs to Mediterranean climate type with  
488 continental and Atlantic influences.

489 The three selected empirical relationships were derived  
490 from ERA-Interim, using daily data for July (representative

of the dry season) and November (representative of the wet  
491 season), by displaying the three pairs of variables in  
492 2D-scattered plots. The reason for the choice of these two  
493 months resides in the considerable differences appearing in  
494 the atmosphere-land surface coupling between dry and  
495 rainy seasons (Betts 2004). The 2D-scattered plots for each  
496 of the three relationships are represented in the upper left  
497 plots of Figs. 5, 6 and 7. They show some differences with  
498 the corresponding plots obtained by Betts (2004) for the  
499 Madeira (Brazil) river basin. These differences are justified  
500 by the fact that they are computed not only with different  
501 re-analysis but geographical location, period, terrain and  
502 weather conditions are also diverse. The largest differences  
503 between Madeira (tropical latitude, south of Equator) and  
504 the Iberian Peninsula (extratropical latitude) are mainly  
505 associated to minimum values of  $SW_{net}$ . Whereas the  
506 minimum value of  $SW_{net}$  in Madeira is approximately the  
507 same in dry and wet seasons, the corresponding minimum  
508 values show a difference of about  $200 \text{ Wm}^{-2}$  in the Iberian  
509 Peninsula. Also, the number of cloudless days is much  
510 higher in the Iberian Peninsula than in Madeira restricting  
511 considerably the  $SW_{net}$  range in the first case.

512 The corresponding relations for each of the RT3-  
513 ENSEMBLES regional simulations are then computed  
514 following the same procedure. Figures 5, 6 and 7 show  
515 2D-scattered plots for the ERA-Interim and for the 13  
516 regional models corresponding to each of the three rela-  
517 tionships for dry (July) and wet (November) seasons.

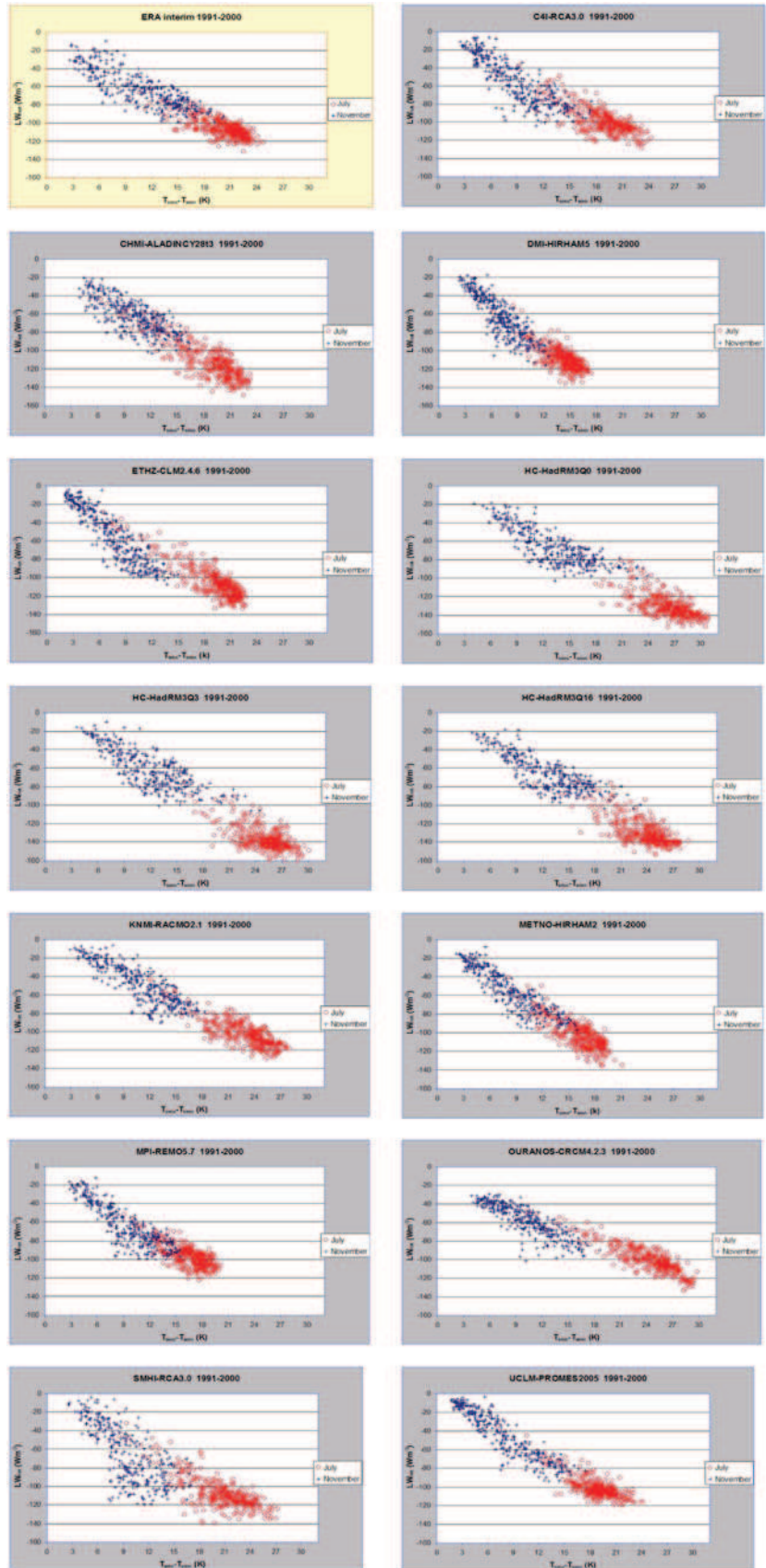
518 Finally, in order to quantify differences or similarities in  
519 the empirical relationships between ERA-Interim and each  
520 one of the 13 regional models, the Hellinger coefficient  
521 (Hellinger 1909) has been used to measure distances of  
522 clouds of points in 2D-scattered plots. The Hellinger  
523 coefficient was originally designed to estimate the prox-  
524 imity of probability density functions (pdf's). The Hellin-  
525 ger coefficient is defined as:

$$d_{\text{Hell}}^{(s)} = \int_{\mathbb{R}} q(x)^s p(x)^{(1-s)} dx, \quad (3)$$

528 where  $q(x)$  and  $p(x)$  are two pdf's to compare, and  $s$  is a  
529 parameter ( $0 < s < 1$ ). The calculation was made choosing  
530  $s = 1/2$  which yields a symmetric measure with values  
531 between zero ( $p$  and  $q$  have disjoint supports) and one ( $p$   
532 and  $q$  are identical). The Hellinger coefficient can be  
533 thought of as measure of the “overlap” between two dis-  
534 tributions. Hellinger coefficient yields information about  
535 differences or similarities in relative position, shape and  
536 orientation of the pdf's. The definition given in Eq. (3) is in  
537 fact a measure of similarity.

538 The kind of evaluation here described is in the same  
539 spirit as those proposed by several authors (Perkins et al.  
540 2007; Perkins and Pitman 2009; Casado and Pastor 2012)

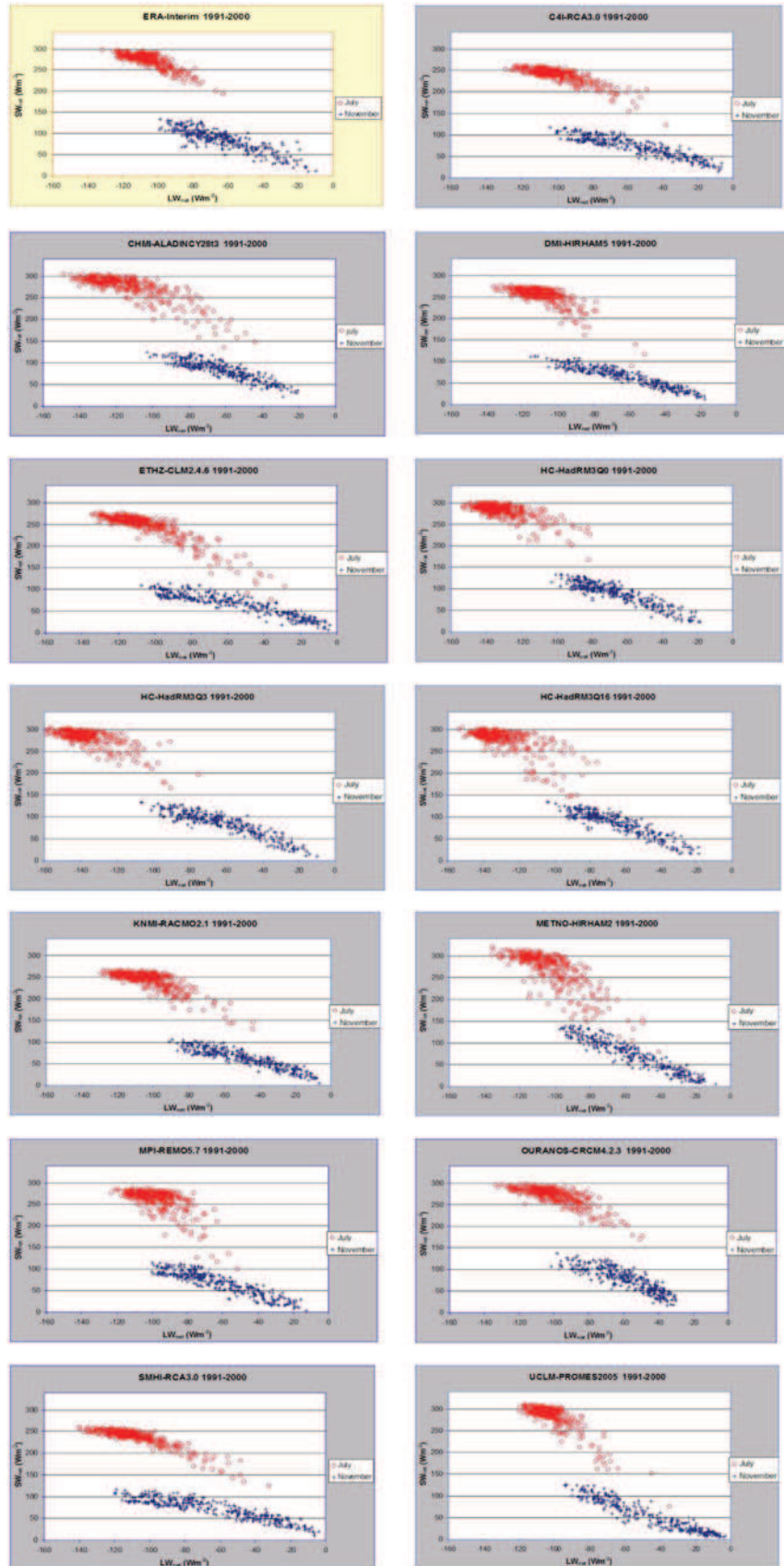
**Fig. 5** Scattered plots of  $LW_{net}$  as a function of  $(T_{smx} - T_{smn})$  for ERA-Interim and thirteen ENSEMBLES RCMs over the selected area. *Red circles* and *blue crosses* correspond to dry (July) and wet (November) seasons, respectively



Author Proof

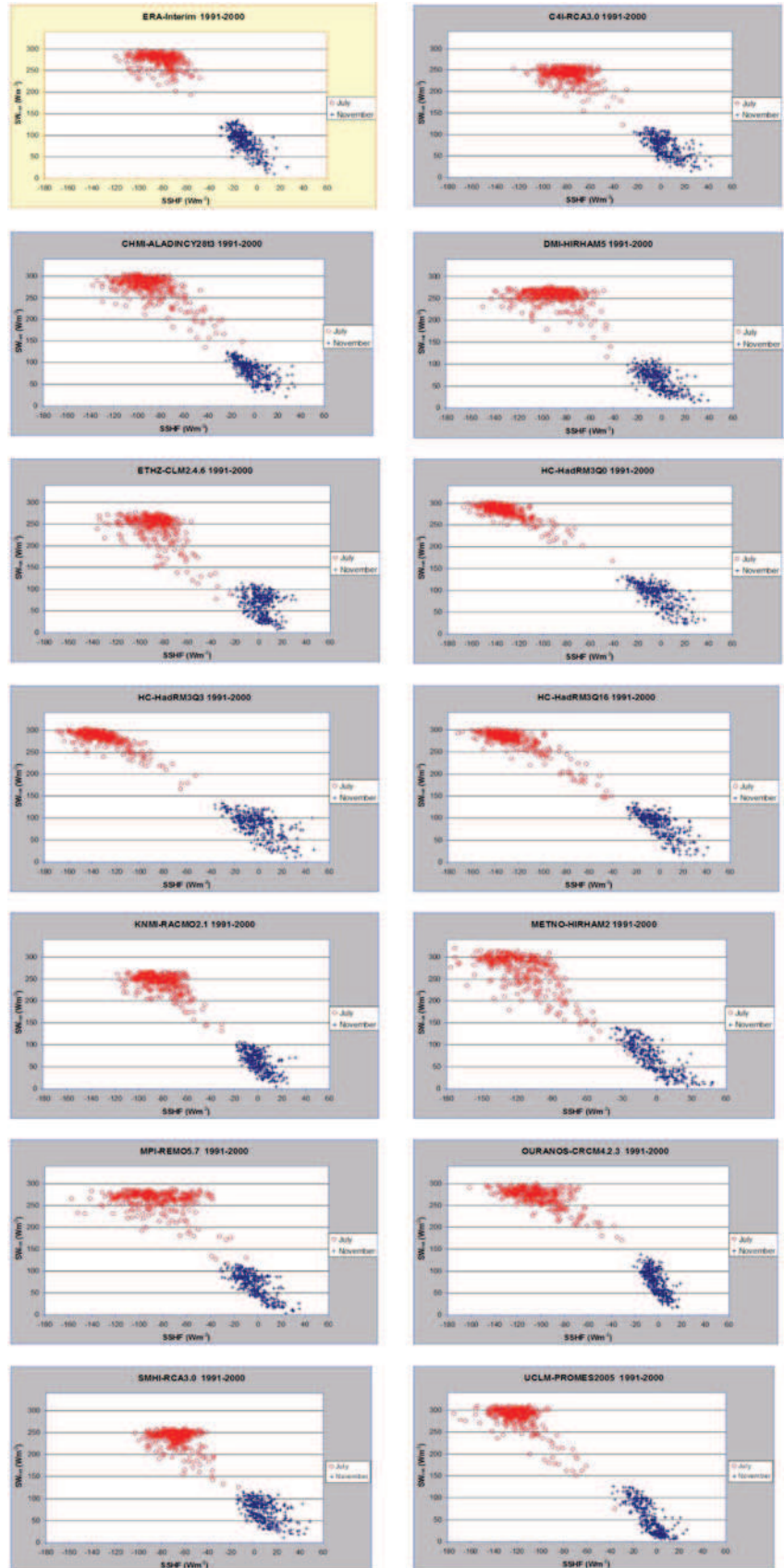


**Fig. 6** The same as Fig. 5, but for  $SW_{net}$  as a function of  $LW_{net}$



Author Proof

**Fig. 7** The same as Fig. 5, but for  $SW_{net}$  as a function SSHF



Author Proof

541 who considered the great advantage of assessing climate  
542 models using metrics derived from pdf's estimated from  
543 daily data.

## 544 5 Results

545 Figure 5 shows the scattered plot of  $LW_{net}$  as a function of  
546 the diurnal range of soil temperature (DTR) for ERA-  
547 Interim and for each of the thirteen RT3-ENSEMBLES  
548 regional models. Points corresponding to July and  
549 November merge in a single quasi-linear distribution for  
550 most models. Other months (not shown here) fall in  
551 between filling in the same distribution. This behaviour  
552 was explained by Betts (2009) that showed that for any  
553 latitude  $DTR \approx -LW_{net} (1/(4\sigma T^3))$ , being  $\sigma$  the Stefan-  
554 Boltzmann constant ( $\sigma = 5.67 \times 10^{-8} \text{ W m}^{-2} \text{ K}^{-4}$ ). A  
555 clear dry atmosphere above causes high values of  $LW_{net}$   
556 and therefore cooling at the surface, leading to lower  
557 minimum surface temperature at night, and a 'stronger'  
558 nocturnal boundary layer (NBL). In terms of daily climate,  
559 this strength of the NBL is closely related to the diurnal  
560 temperature range  $DTR = T_{max} - T_{min}$ . Most of the plots  
561 show that the range of DTR is roughly double for  
562 November (wet season) as compared to July (dry season).  
563  $LW_{net}$  also shows higher values for the wet season as  
564 compared to dry season. The reasons for such higher values  
565 of  $LW_{net}$  during the wet season reside principally in the  
566 usually greater cloud cover and higher lifting condensation  
567 level (LCL). From a daily climate perspective, day-time  
568 and night-time boundary layers are a fully coupled system,  
569 frequently being a deep residual mixed layer from the  
570 previous day.  $LW_{net}$  is usually correlated with the strength  
571 of NBL and the thickness of the diurnal boundary layer.

572 The maximum upward  $LW_{net}$  for ERA-Interim in July  
573 reaches a value of about  $-130 \text{ W m}^{-2}$ . The corresponding  
574 RCMs values for these maxima are highly variable,  
575 reaching values up to  $-160 \text{ W m}^{-2}$  (for HadRM3 model).  
576 In the month of November, maximum values of  $LW_{net}$  are  
577 of about  $-100 \text{ W m}^{-2}$  for all models (including ERA-  
578 Interim) except for SMHI-RCA and DMI-HIRHAM where  
579 maximum values rise up to  $-120 \text{ W m}^{-2}$  (see Fig. 5).  
580 These maxima correspond to clear days with low atmo-  
581 spheric humidity.

582 Figure 6 depicts the scattered plot of  $SW_{net}$  as a function  
583 of  $LW_{net}$ , showing two well differentiated distributions for  
584 July and November. The scattered plot corresponding to  
585 ERA-Interim suggests that  $SW_{net}$  and  $LW_{net}$  are coupled  
586 only in the few cloudy days of the month of July. However,  
587 no coupling seems to exist in clear days which are majority  
588 in July. None of the RCM seems to properly simulate this  
589 behaviour. Differences in the upper limits of  $SW_{net}$  of up to  
590  $30 \text{ W m}^{-2}$  between ERA-Interim and some RCMs might be

due to different surface albedo. In November where clear  
591 days are infrequent, coupling between  $SW_{net}$  and  $LW_{net}$  is  
592 not so tight possibly caused by advection of atmospheric  
593 water vapour. Differences between RCMs and ERA-  
594 Interim are smaller in November than in July, showing  
595 several RCMs stronger  $SW_{net} - LW_{net}$  coupling than for  
596 ERA-Interim.

597 The scattered plot of  $SW_{net}$  as a function of SSHF based  
598 on ERA-Interim (see Fig. 7) shows almost no coupling  
599 between  $SW_{net}$  and SSHF for the month of July. The sur-  
600 face energy budget equation (see Eq. 1) can be conse-  
601 quently simplified as  $R_{net} = SW_{net} + LW_{net} = SSHF$  due  
602 to the lack of available water for evapotranspiration during  
603 dry season. Therefore, most of the net surface radiation,  
604  $R_{net}$ , will turn back as SSHF to the atmosphere, favouring  
605 the coupling  $SSHF - LW_{net}$  and preventing the coupling  
606  $SSHF - SW_{net}$ . On the other hand, the month of Novem-  
607 ber (wet season) shows a clear  $SW_{net} - SSHF$  coupling.  
608 Some RCMs show greater coupling than ERA-Interim in  
609 cloudy July days. The behaviour of RCMs in November is  
610 highly variable as compared with ERA-Interim.

611 Table 2 summarizes Hellinger distances between ERA-  
612 Interim and each one of the ENSEMBLES RCMs and for  
613 each of the three selected relations describing the atmo-  
614 sphere-land surface coupling for July and November. The  
615  $T2m - PP$  relationship has also been added for the sake of  
616 comparison with previous studies (e.g., Christensen et al.  
617 2010). Hellinger coefficients for July tend to be smaller  
618 than the corresponding values for November, meaning that  
619 coupling in dry season is worse simulated than in wet  
620 season. This effect is particularly clear for the relation  
621  $SW_{net} - SSHF$ . Tables 3 and 4 summarize for July and  
622 November standard skill scores between ERA-Interim and  
623 each one of the ENSEMBLES RCMs for 2-m Temperature  
624 and Daily Total Precipitation, respectively.

625 There is an overall agreement of temperature skill  
626 scores—including Hellinger coefficient for  $T2m - PP$ —  
627 discriminating consistently best and worst models (see  
628 Table 3). For example, KNMI-RACMO model in July is  
629 ranked respectively as second, first, first, fourth and first  
630 best model when using the following performance metrics:  
631 bias, mean absolute error, RMSE, correlation coefficient  
632 and Hellinger coefficient for  $T2m - PP$ . Also, HadRM3Q3  
633 model in July is ranked as the worst model when using  
634 bias, mean absolute error and RMSE and the second and  
635 third worst when using correlation coefficient and Hellin-  
636 ger coefficient for  $T2m - PP$ , respectively.

637 Tables 3 and 4 clearly show that models performing  
638 well in 1 month and for one variable not necessarily they  
639 do in other months and variables. This fact is well known  
640 and it is a direct consequence of the predominance of  
641 certain processes in one or another season affecting more to  
642 one or another variable. For example, temperature in  
643

**Table 2** Values of Hellinger coefficient for the relations  $LW_{net} - (T_{smx} - T_{smn})$ ,  $SW_{net} - LW_{net}$ ,  $SW_{net} - SSHF$  and  $T2m - PP$  for the months of July and November

Institution-model	Hellinger coefficient July				Hellinger coefficient November			
	$LW_{net} - (T_{smx} - T_{smn})$	$SW_{net} - LW_{net}$	$SW_{net} - SSHF$	$T2m - PP$	$LW_{net} - (T_{smx} - T_{smn})$	$SW_{net} - LW_{net}$	$SW_{net} - SSHF$	$T2m - PP$
CHMI-ALADIN	0.86	0.83	<b>0.85</b>	0.84	0.96	0.99	<b>0.93</b>	0.98
C4I-RCA3	0.91	0.58	0.61	0.94	0.94	0.94	0.78	0.96
DMI-HIRHAM	0.39	0.85	0.79	0.93	<u>0.78</u>	0.91	0.85	<b>1.00</b>
ETHZ-CLM	0.88	0.70	0.74	0.86	0.85	0.90	<u>0.76</u>	0.99
METO-HC_HadRM3Q0	0.30	0.59	<u>0.25</u>	0.96	0.95	0.99	<b>0.93</b>	0.98
METO-HC_HadRM3Q3	<u>0.28</u>	<u>0.43</u>	0.28	0.84	<b>0.99</b>	<b>1.00</b>	0.88	0.98
METO-HC_HadRM3Q16	0.55	0.62	0.47	0.92	0.98	<b>1.00</b>	0.89	0.99
KNMI-RACMO	0.86	0.70	0.72	<b>0.99</b>	0.94	0.84	0.77	0.94
METNO-HIRHAM	0.71	0.79	0.51	0.92	0.91	0.93	0.84	0.96
MPI-M-REMO	0.69	0.84	0.81	0.95	0.96	0.95	0.89	0.98
SMHI-RCA	0.92	0.59	0.54	0.89	0.92	0.92	0.78	0.94
OURANOS-CRCM	0.75	<b>0.93</b>	0.77	<u>0.71</u>	0.96	0.97	0.87	<u>0.90</u>
UCLM-PROMES	<b>0.94</b>	0.89	0.40	–	0.86	<u>0.80</u>	0.85	–

The RCM acquiring the **highest** and the lowest respective value for each relation is indicated

**Table 3** Bias, mean absolute error, root mean square error and correlation coefficient for 2-m Temperature

Institution-model	2-m Temperature July				2-m Temperature November			
	Bias	MAE	RMSE	Corr. Coeff.	Bias	MAE	RMSE	Corr. Coeff.
CHMI-ALADIN	1.23	1.29	1.63	0.92	<u>2.51</u>	<u>2.59</u>	<u>2.78</u>	0.91
C4I-RCA3	1.15	1.50	1.82	0.87	1.70	1.92	2.28	0.86
DMI-HIRHAM	–1.01	1.15	1.38	<b>0.94</b>	<b>0.11</b>	<b>0.73</b>	<b>0.94</b>	<b>0.94</b>
ETHZ-CLM	–1.07	1.33	1.52	<b>0.94</b>	0.81	1.14	1.38	0.93
METO-HC_HadRM3Q0	–1.61	2.02	2.51	0.76	1.02	1.60	2.06	<u>0.79</u>
METO-HC_HadRM3Q3	<u>–3.16</u>	<u>3.24</u>	<u>3.96</u>	0.66	0.82	1.43	1.88	0.81
METO-HC_HadRM3Q16	–2.15	2.42	3.08	0.70	0.81	1.47	1.85	0.82
KNMI-RACMO	0.70	<b>0.95</b>	<b>1.26</b>	0.93	1.84	1.95	2.24	0.90
METNO-HIRHAM	–1.34	1.73	2.17	0.84	0.25	1.04	1.30	0.89
MPI-M-REMO	–1.38	1.53	1.79	0.92	–0.48	0.91	1.21	0.92
SMHI-RCA	1.74	1.77	1.98	<b>0.94</b>	2.08	2.18	2.54	0.88
OURANOS-CRCM	2.47	2.45	2.87	0.87	2.36	2.48	2.73	0.89
UCLM-PROMES	<b>–0.25</b>	1.83	2.38	<u>0.64</u>	1.63	1.38	2.38	0.80

644 summertime is very much related with the correct partition  
 645 of sensible and latent heat fluxes, which in turn depends on  
 646 a reasonable simulation of soil water content. This is not  
 647 the case in wintertime. Finally, Table 5 displays eight  
 648 different rankings of the 13 ENSEMBLES RCMs accord-  
 649 ing to the value of the Hellinger coefficient for each of the  
 650 four considered relationships computed for the months of  
 651 July and November. It is noticeable that for November  
 652 there is a high consistency among rankings based on the  
 653 here considered relationships. This consistency implies that  
 654 one could use fewer relationships to select the models

655 better simulating atmosphere-land surface coupling. How-  
 656 ever, discrepancy among different models rankings—  
 657 depending on the chosen relation—is higher for July,  
 658 possibly due to the different quality of radiation fluxes and  
 659 heat fluxes. It is also noticeable the large differences  
 660 appearing between dry and wet seasons in the rankings. It  
 661 is very significant that some models highly scored for the  
 662 wet season only get poor scores for the dry season and vice  
 663 versa.

664 Now, at this point, question arises whether a ranking of  
 665 models based on standard skill scores for 2-m Temperature

**Table 4** The same as Table 3, but for Daily Total Precipitation

Institution-model	Daily total precipitation July				Daily total precipitation November			
	Bias	MAE	RMSE	Corr. Coeff.	Bias	MAE	RMSE	Corr. Coeff.
CHMI-ALADIN	-0.34	0.38	1.10	0.79	-0.51	0.83	1.84	<b>0.94</b>
C4I-RCA3	-0.20	0.31	0.81	0.62	-0.45	1.06	2.19	0.87
DMI-HIRHAM	<b>0.00</b>	<b>0.19</b>	0.74	0.78	-0.07	0.83	1.99	0.90
ETHZ-CLM	-0.13	0.26	1.11	0.66	-0.15	<b>0.74</b>	<b>1.66</b>	0.92
METO-HC_HadRM3Q0	-0.08	0.31	0.76	0.37	<b>-0.05</b>	0.92	2.31	<u>0.86</u>
METO-HC_HadRM3Q3	-0.01	0.26	0.73	0.30	-0.25	0.96	2.38	0.88
METO-HC_HadRM3Q16	-0.07	0.32	0.89	<u>0.23</u>	<b>-0.05</b>	0.89	2.24	0.87
KNMI-RACMO	0.05	<b>0.19</b>	0.72	0.50	-0.40	0.84	2.09	0.90
METNO-HIRHAM	-0.08	0.22	<b>0.69</b>	<b>0.81</b>	<u>-0.89</u>	<u>1.18</u>	<u>3.17</u>	0.89
MPI-M-REMO	-0.17	0.28	0.75	0.57	-0.24	0.82	2.39	0.89
SMHI-RCA	-0.14	0.26	0.82	0.76	-0.35	0.85	1.68	0.92
OURANOS-CRCM	<u>-0.99</u>	<u>0.98</u>	<u>1.70</u>	0.63	-0.07	1.00	1.87	0.90

**Table 5** Rankings of 13 ENSEMBLES RCMs (in numbers) according to Hellinger coefficient based on the proximity of the relationships:  $LW_{net} - (T_{smx} - T_{snn})$ ,  $SW_{net} - LW_{net}$ ,  $SW_{net} - SSHF$ , and  $T2m - PP$  for the months of July and November

Institution-model	July				November			
	$LW_{net} - (T_{smx} - T_{snn})$	$SW_{net} - LW_{net}$	$SW_{net} - SSHF$	$T2m - PP$	$LW_{net} - (T_{smx} - T_{snn})$	$SW_{net} - LW_{net}$	$SW_{net} - SSHF$	$T2m - PP$
CHMI-ALADIN	6	5	<b>1</b>	10	4	4	<b>1</b>	7
C4I-RCA3	3	12	7	4	7	7	10	9
DMI-HIRHAM	11	3	3	5	<u>13</u>	10	7	<b>1</b>
ETHZ-CLM	4	7	5	9	12	11	<u>13</u>	2
HC-HadRM3Q0	12	10	<u>13</u>	2	6	3	2	5
HC-HadRM3Q3	<u>13</u>	<u>13</u>	12	11	<b>1</b>	<b>1</b>	5	6
HC-HadRM3Q16	10	9	10	6	2	2	3	3
KNMI-RACMO	5	8	6	<b>1</b>	8	12	12	10
METNO-HIRHAM	8	6	9	7	10	8	9	8
MPI-REMO	9	4	2	3	5	6	4	4
SMHI-RCA	2	11	8	8	9	9	11	11
OURANOS-CRCM	7	<b>1</b>	4	<u>12</u>	3	5	6	<u>12</u>
UCLM-PROMES	<b>1</b>	2	11	-	11	<u>13</u>	8	-

666 and Daily Total Precipitation would be consistent with a  
 667 ranking based on Hellinger coefficients as it is here pro-  
 668 posed. And provided that consistency of results holds, what  
 669 would an evaluation based on Hellinger coefficients add to  
 670 the more traditional approach based on skill scores for  
 671 temperature and precipitation? Results summarized in  
 672 Tables 2, 3, 4 and 5 allow us to conclude that not always  
 673 models best/worst performing in terms of standard scores  
 674 for temperature and precipitation show consistent perfor-  
 675 mance in terms of Hellinger coefficients for the pairs of  
 676 quantities here selected. As an example, the outstanding  
 677 performance of KNMI-RACMO model in July for tem-  
 678 perature (see Table 3) has not counterpart in terms of

679 Hellinger coefficients (see Table 5). This can be explained  
 680 by the fact that the overall surface energy budget is rea-  
 681 sonably well captured although individual fluxes might not  
 682 be properly simulated. On the other hand, the deficient  
 683 performance of HadRM3Q3 model in July for temperature  
 684 is also confirmed in terms of Hellinger coefficients. In  
 685 November consistency among standard scores for temper-  
 686 ature and Hellinger coefficients is less clear. This may be  
 687 justified by the fact that local wintertime (heat and radia-  
 688 tion) fluxes are not so strong and consequently 2-m Tem-  
 689 perature is also affected by other non-local factors.

690 The comparison of our results with those of Christensen  
 691 et al. (2010) is not straightforward for a number of reasons.

692 First, their work was aiming to merge a collection of 6  
693 performance metrics into an aggregated model weight with  
694 the purpose of combining climate change information from  
695 the range of RCMs. They proposed 3 different ways of  
696 combining the 6 performance metrics showing a relatively  
697 high degree of coincidence for the final weight. Second, the  
698 purpose of their work was to get a single valued model  
699 weight describing the overall performance of each RCM  
700 for the whole domain, for all seasons and for all considered  
701 variables. Contrary, our work does not intend to generate  
702 an overall performance score. We have instead attempted  
703 to propose some scores based on the Hellinger coefficient  
704 determining how well atmosphere-land surface coupling is  
705 simulated by models. Furthermore, this evaluation scores  
706 may help to detect problems which may be behind a poor  
707 model performance in terms of temperature and precipi-  
708 tation. Nevertheless, some coincidences appear in the  
709 results based on both approaches.

710 Therefore, we have preferred not to merge the obtained  
711 eight rankings into just one ranking in order to highlight  
712 how differences among rankings depend strongly on season  
713 and to a lesser extent on the particular relationship  
714 expressing the atmosphere-land surface coupling. We  
715 confirm with our results that model rankings are highly  
716 dependent on region, variables, seasons and metrics  
717 selected for the evaluation in full agreement with other  
718 authors (e.g., Knutti et al. 2010; Casado and Pastor 2012).

## 719 6 Conclusions

720 An original approach has been proposed for evaluating  
721 regional climate models based on the comparison of  
722 empirical relationships among model outcome variables.  
723 The proposed method provides tools to identify which  
724 processes related to the atmosphere-land surface coupling  
725 are not properly simulated by models. Contrary to more  
726 classical methods essentially focused on traditional climate  
727 variables—like air temperature and precipitation—here the  
728 focus is put on fluxes which are in the end terms appearing  
729 in the budget equations determining temperature and soil  
730 moisture. Soil moisture is responsible for the right partition  
731 of surface energy between latent and sensible heat fluxes,  
732 and in turn of the structure of boundary layer in terms of  
733 temperature and humidity. The approach provides a  
734 quantitative evaluation of models and therefore allows the  
735 establishment of model rankings focusing on the ability to  
736 properly simulate the interaction between atmosphere and  
737 land surface. Thirteen RCMs participating in the  
738 ENSEMBLES project were selected by the availability of  
739 daily data for the period 1991–2000 of the variables  $LW_{net}$ ,  
740  $SW_{net}$ , SSHF, T<sub>max</sub> and T<sub>min</sub>. Three pairs of relations  
741 among surface energy variables and fluxes relevant to the

energy and water budget were obtained for an area cov- 742  
ering part of two river basins within southern Iberian 743  
Peninsula and for 2 months representative of the dry and 744  
wet seasons, respectively. The truth to compare with model 745  
simulations was ERA-Interim re-analysis. As it was 746  
already mentioned in Sect. 1, the comparison of RCMs 747  
against ERA-Interim may have certain flaws mainly when 748  
comparing variables not directly observed, as it is the case 749  
for the fluxes. However, comparison of ERA-Interim fluxes 750  
against satellite estimations allow us to conclude that ERA- 751  
Interim fluxes have a reasonable quality to be used as 752  
ground truth reference. Our main aim, however, was to 753  
illustrate the value of comparing magnitudes representative 754  
of certain processes in order to quantify how well models 755  
are capturing them. Besides, significant deviation of some 756  
models for certain magnitudes and seasons can help to 757  
identify problems when simulating processes as complex as 758  
those responsible for the atmosphere-land surface coupling. 759  
The Hellinger coefficient was the metric selected to 760  
quantify the distance between each of the regional models 761  
and the reference represented by ERA-Interim. 762

763 The comparison of the relationships here obtained for  
764 southern Iberian Peninsula with those obtained by Betts  
765 (2004) for the Madeira basin (Brazil) confirms that such  
766 comparison is highly dependent on season, region and cli-  
767 mate conditions. In that sense, this approach is very adequate  
768 to quantify the regional performance of climate models.

769 The proximity of modelled and reference scattered plots  
770 depends very much on the season. The generally higher  
771 value of Hellinger coefficient (lower distance) for the wet  
772 season is indicative of difficulties associated with the  
773 simulation of atmosphere-land surface coupling during the  
774 dry season. Moreover, the high coincidence of the four  
775 rankings for the wet season suggests that only one relation  
776 may be enough to discriminate the “best” and “worst”  
777 models at that time of the year. This is not the case for the  
778 dry season, where more relations seem to be needed to  
779 quantify the radiative and water aspects of modelled sur-  
780 face coupling. The range of Hellinger coefficient values  
781 tends to be narrower in the wet season showing a high  
782 degree of agreement among different model simulations in  
783 coincidence with results by Betts et al. (2006).

784 We would like to point out that most methods for  
785 evaluating climate models frequently put the focus on  
786 outcome variables (usually precipitation and temperature)  
787 disregarding important aspects related to the coupling  
788 between subsystems of the climate system. We are con-  
789 vinced of the importance of evaluation studies focusing on  
790 physical processes, and in particular on the features of  
791 interface between subsystems. In this line, our approach  
792 aims directly at the performance of models in connection  
793 with the atmosphere-land surface interaction which is in  
794 the end highly responsible for a realistic simulation of

795 variables more commonly described in climate studies,  
796 such as precipitation and temperature.

797 We may conclude by saying that the here proposed  
798 method of evaluating RCMs does not only intend to present  
799 an additional set of performance-based metrics aiming to  
800 rank models or to weight them within an ensemble of  
801 RCMs as it was proposed by other authors (e.g., Chris-  
802 tensen et al. 2010). Our proposal goes mainly in the  
803 direction of exploring and quantifying how well coupling  
804 between atmosphere-land surface is simulated by different  
805 RCMs. As we mentioned in the introduction, climate  
806 models are based on sound and well established physical  
807 laws and their success in simulating the climate system  
808 depends on an accurate representation of the climate rele-  
809 vant processes. Consequently, our proposal of evaluation  
810 heavily relies on physical processes—and in this particular  
811 case on interaction between subsystems—instead of the  
812 more traditional methods which are more focused on the  
813 behaviour of climate variables such as temperature and  
814 precipitation. Additionally, the analysis of the simulated  
815 coupling between subsystems could help to diagnose  
816 modelling deficiencies which may be behind a poor per-  
817 formance in terms of climate variables.

818 **Acknowledgments** The ENSEMBLES data used in this work was  
819 funded by the EU FP6 Integrated Project ENSEMBLES (Contract  
820 number 505539) whose support is gratefully acknowledged by the  
821 authors of the paper, without these data it would have been impossible  
822 to write this article. We also thank DWD and ECMWF for providing  
823 Climate Monitoring SAF (CM SAF) and ERA-Interim re-analysis  
824 datasets, respectively. Special thanks are also due to our colleagues  
825 M.J. Casado, M.A. Pastor, J.A. López, J.A. García-Moya and  
826 B. Navascués for their fruitful suggestions. Finally, we thank to two  
827 anonymous referees who have substantially contributed with their  
828 constructive comments to the final form of this work.

## 829 References

- 830 Baldocchi D, Falge E, Gu L, Olson R, Hollinger D, Running S,  
831 Anthoni P, Bernhofer Ch, Davis K, Evans R et al (2001)  
832 FLUXNET: a new tool to study the temporal and spatial  
833 variability of ecosystem-scale carbon dioxide. *Bull Am Meteorol*  
834 *Soc* 82:2415–2434
- 835 Betts AK (2004) Understanding hydrometeorology using global  
836 models. *Bull Am Meteorol Soc* 85:1673–1688. doi:10.1175/  
837 BAMS-85-11-1673
- 838 Betts AK (2007) Coupling of water vapor convergence, clouds,  
839 precipitation, and land-surface processes. *J Geophys Res* 112:  
840 D10108. doi:10.1029/2006JD008191
- 841 Betts AK (2009) Land surface-atmosphere coupling in observations  
842 and models. *J Adv Model Earth Syst* 1, Art.#4, 18 pp, doi:  
843 10.3894/JAMES.2009.1.4
- 844 Betts AK, Ball J, Barr A, Black TA, McCaughey JH, Viterbo P (2006)  
845 Assessing land-surface-atmosphere coupling in the ERA-40  
846 reanalysis with boreal forest data. *Agric For Meteorol*  
847 140:355–382. doi:10.1016/j.agrformet.2006.08.009
- 848 Böhm U, Küchen M, Ahrens W, Block A, Hauffe D, Keuler K,  
849 Rockel B, Will A (2006). CLM-the climate version of LM: brief  
description and long-term applications. COSMO Newsletter No  
6 850  
851
- Casado MJ, Pastor MA (2012) Use of variability modes to evaluate  
AR4 climate models over the Euro-Atlantic region. *Clim Dyn*  
38:225–237. doi:10.1007/s00382-011-1077-2 852  
853  
854
- CCSP (2008) Climate models: an assessment of strengths and  
limitations. A report by the U.S. Climate Change Science  
Program and the Subcommittee on Global Change Research  
[Bader D.C., C. Covey, W.J. Gutowski Jr., I.M. Held, K.E.  
Kunkel, R.L. Miller, R.T. Tokmakian and M.H. Zhang  
(Authors)]. Department of Energy, Office of Biological and  
Environmental Research, Washington, D.C., USA, 124 pp 855  
856  
857
- Christensen JH, Christensen OB (2007) A summary of the PRU-  
DENCE model projections of changes in European climate by  
the end of this century. *Clim Change* 81(Suppl 1):7–30 858  
859  
860
- Christensen JH, Kjellström E, Giorgi F, Lenderink G, Rummukainen  
M (2010) Weight assignment in regional climate models. *Clim*  
*Res* 44:179–194 861  
862  
863
- Collins M, Booth BBB, Harris GR, Murphy JM, Sexton DMH, Webb  
MJ (2006) Towards quantifying uncertainty in transient climate  
change. *Clim Dyn* 27:127–147. doi:10.1007/s00382-006-0121-0 864  
865  
866
- Cramer H (1946) Mathematical methods of statistics. Princeton  
University Press, Princeton, p 354 867  
868  
869
- Dee DP et al (2011) The ERA-Interim reanalysis: configuration and  
performance of the data assimilation system. *Q J R Meteorol Soc*  
137:553–597. doi:10.1002/qj.828 870  
871  
872
- Déqué M, Jones RG, Wild M, Giorgi F et al (2005) Global high  
resolution versus limited area model climate change projections  
over Europe: quantifying confidence level from PRUDENCE  
results. *Clim Dyn* 25:653–670 873  
874  
875
- Déqué M, Rowell DP, Lüthi D, Giorgi F et al (2007) An  
intercomparison of regional climate simulations for Europe:  
assessing uncertainties in model projections. *Clim Change*  
81(Suppl 1):53–70 876  
877  
878
- Douville H, Mahfouf J-F, Saarinen S, Viterbo P (1998) The ECMWF  
surface analysis: diagnostics and prospects. Tech. Memo. No.  
258. ECMWF, Reading, UK 879  
880  
881
- Douville H, Viterbo P, Mahfouf J-F, Beljaars ACM (2000) Evaluation of  
the optimum interpolation and nudging techniques for soil moisture  
analysis using FIFE data. *Mon Weather Rev* 128:1733–1756 882  
883  
884
- Garratt JR (1992) The atmospheric boundary layer. Cambridge  
University Press, Cambridge, p 316 885  
886  
887
- Giorgi F, Mearns LO (2002) Calculation of average, uncertainty  
range, and reliability of regional climate changes from AOGCM  
simulations via the Reliability Ensemble Averaging (REA)  
method. *J Clim* 15:1141–1158 888  
889  
890
- Gleckler PJ, Taylor KE, Doutriaux C (2008) Performance metrics for  
climate models. *J Geophys Res* 113:D06104. doi:10.1029/  
2007JD008972 891  
892  
893
- Haugen JE, Haakensatd H (2006) Validation of HIRHAM version  
with 50 km and 25 km resolution. RegClim General Technical  
Report, No. 9, pp 159–173 894  
895  
896
- Hellinger E (1909) Neue Begründung der Theorie quadratischer  
Formen von unendlich vielen Veränderlichen. *J Reine Angew*  
*Math* 136:210–271 897  
898  
899
- Jacob D (2001) A note to the simulation of the annual and inter-  
annual variability of the water budget over the Baltic Sea  
drainage basin. *Meteorol Atmos Phys* 77:61–73 900  
901  
902
- Jaeger EB, Stöckli R, Seneviratne SI (2009) Analysis of planetary  
boundary fluxes and land-atmosphere coupling in the regional  
climate model CLM. *J Geophys Res* 114:D17106 903  
904  
905
- Kjellström E, Giorgi F (2010) Regional climate model evaluation and  
weighting, introduction. *Clim Res* 44:117–119. doi:10.3354/  
cr00976 906  
907  
908
- Kjellström E, Bärring L, Gollvik S, Hansson U, Jones C, Samuelsson  
P, Rummukainen M, Ullersig A, Willen U, Wyser K (2005) A  
909  
910  
911  
912  
913  
914  
915

- 916 140-year simulation of European climate with the new version of  
917 the Rossby Centre regional atmospheric climate model (RCA3).  
918 Reports Meteorology and Climatology, 108, SMHI, SE-60176  
919 Norrköping, Sweden, 54 pp
- 920 Knutti R, Furrer R, Tebaldi C, Cermak J, Meehl GA (2010)  
921 Challenges in combining projections from multiple climate  
922 models. *J Clim* 23:2739–2758. doi:10.1175/2009JCLI3361.1
- 923 Král T (2011) Flux tower observations for the evaluation of land  
924 surface schemes: application to ERA-Interim. ERA report series  
925 No 11. ECMWF, Shinfield Park, Reading, RG2 9AX, England
- 926 Mahfouf J-F, Viterbo P, Douville H, Beljaars ACM, Saarinen S  
927 (2000) A revised land-surface analysis scheme in the integrated  
928 forecasting system. *ECMWF Newsl* 88:8–13
- 929 Mearns LO, Giorgi F, Whetton P, Pabon D, Hulme M, and Lal M  
930 (2003) Guidelines for use of climate scenarios developed from  
931 regional climate model experiments. Data distribution centre of  
932 the international panel of climate change, 38 pp. (Available for  
933 download from [www.ipcc-data.org/guidelines/dgm\\_no1\\_v1\\_10-2003.pdf](http://www.ipcc-data.org/guidelines/dgm_no1_v1_10-2003.pdf))
- 934 Perkins SE, Pitman AJ (2009) Do weak AR4 models bias projections  
935 of future climate changes over Australia?. *Clim Change*  
936 93:527–558
- 937 Perkins SE, Pitman AJ, Holbrook NJ, McAneney J (2007) Evaluation  
938 of the AR4 climate models simulated daily maximum temper-  
939 ature, minimum temperature, and precipitation over Australia  
940 using probability density functions. *J Clim* 20:4356–4376
- 941 Plummer D, Caya D, Coté H, Frigon A, Biner S, Giguère M, Paquin  
942 D, Harvey R, de Elia R (2006) Climate and climate change over  
943 North America as simulated by the canadian regional climate  
944 model. *J Clim* 19:3112–3132
- 945 Randall DA, Wood RA, Bony S, Coleman R, Fichefet T, Fyfe J,  
946 Kattsov V, Pitman A, Shukla J, Srinivasan J, Stouffer RJ, Sumi  
947 A, Taylor KE (2007) Climate models and their evaluation,  
948 chapter of the book climate change 2007: the physical science  
949 basis. In: Solomon S, Qin D, Manning M, Chen Z, Marquis M,  
950 Averyt KB, Tignor M, Miller HL (eds) Contribution of working  
951 group I to the fourth assessment report of the intergovernmental  
952 panel on climate change. Cambridge University Press, Cam-  
953 bridge, pp 589–662
- 954 Sánchez E, Gallardo C, Gaertner MA, Arribas A, Castro M (2004)  
955 Future climate extreme events in the Mediterranean simulated by  
956 a regional climate model: a first approach. *Global Planet Change*  
44:163–180
- Santanello JA Jr, Peters-Lidard CD, Kumar SV, Alonge C, Tao WK  
(2009) A modeling and observational framework for diagnosing  
local land-atmosphere coupling on diurnal time scales. *J Hydro-  
meteorol* 10(3):577–599
- Schmidli J, Goodess CM, Frei C, Haylock MR, Hündecha Y,  
Ribalaygua J, Schmith T (2007) Statistical and dynamical  
downscaling of precipitation: an evaluation and comparison of  
scenarios for the European Alps. *J Geophys Res* 112:D04105.  
doi:10.1029/2005JD007026
- Seneviratne SI, Corti T, Davin E, Hirschi M, Jaeger EB, Lehner I,  
Orlowsky B, Teuling AJ (2010) Investigating soil moisture-  
climate interactions in a changing climate: a review. *Earth-Sci*  
*Rev* 99(3–4):125–161. doi:10.1016/j.earscirev.2010.02.04
- Stensrud DJ (2007) Parameterization schemes: keys to understanding  
numerical weather prediction models. Cambridge University  
Press. ISBN: 9780521865401, 459 p
- Uppala SM, Källberg PW, Simmons AJ, Andrae U, da Costa Bechtold  
V, Fiorino M, Gibson JK, Haseler J, Hernandez A, Kelly GA, Li  
X, Onogi K, Saarinen S, Sokka N, Allan RP, Andersson E, Arpe  
K, Balmaseda MA, Beljaars ACM, van de Berg L, Bidlot J,  
Bormann N, Caires S, Chevallier F, Dethof A, Dragosavac M,  
Fisher M, Fuentes M, Hagemann S, Hölm E, Hoskins BJ, Isaksen  
L, Janssen PAEM, Jenne R, McNally AP, Mahfouf JF, Morcrette  
JJ, Rayner NA, Saunders RW, Simon P, Sterl A, Trenberth KE,  
UnCTh A, Vasiljevic D, Viterbo P, Woollen J (2005) The ERA-  
40 re-analysis. *Q J R Meteorol Soc* 131:2961–3012. doi:10.1256/  
qj.04.176
- van der Linden P, Mitchell JFB (eds) (2009) ENSEMBLES: climate  
change and its impacts. Summary of research and results from  
the ENSEMBLES project. Met Office Hadley Centre, Exeter
- Van Meijgaard et al (2008) Simulation of present day climate in  
RACMO2: first results and model developments. Technical  
report No 252, KNMI, 24 pp
- Wilby RL, Charles SP, Zorita E, Timbal B, Whetton P, Mearns LO  
(2004). Guidelines for use of climate scenarios developed from  
statistical downscaling method. Data Distribution centre of the  
international panel of climate change, 27 pp. (Available for  
download from [www.ipcc-data.org/guidelines/dgm\\_no2\\_v1\\_09-2004.pdf](http://www.ipcc-data.org/guidelines/dgm_no2_v1_09-2004.pdf))